

Fig.2 Measurement diagram

Table I Experimental parameters

Parameters	Values
Yield shear force coefficient C_y	0.248, 0.314, 0.413, 0.612, ∞
Coefficient of dynamic friction μ_d	0.100, 0.188, 0.435, ∞
Maximum velocity V_{max} (m/s)	0.2, 0.3, 0.4, 0.5
Mass ratio R_m	0.219, 0.438, 0.657

* Boxes indicate reference values

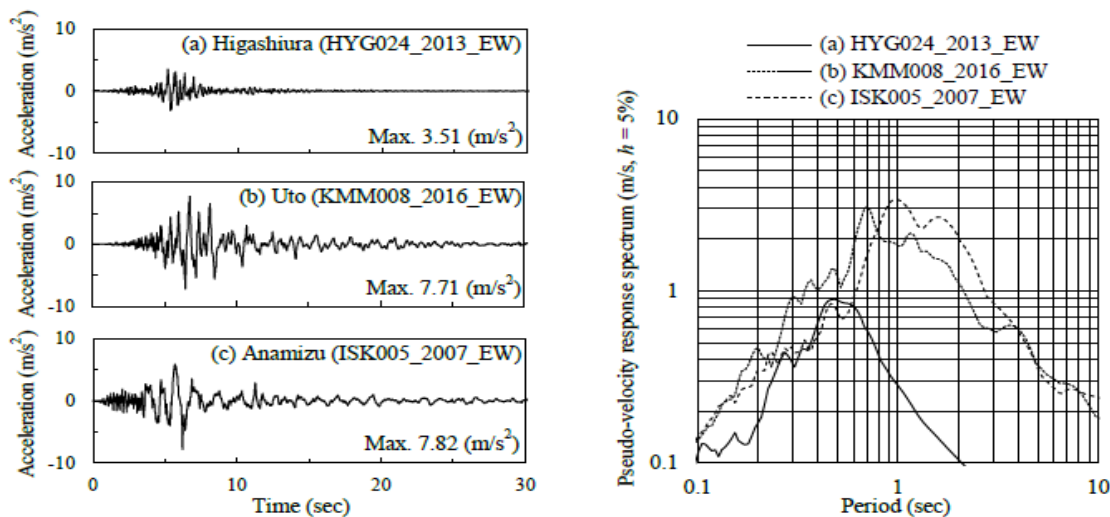


Fig.3 Acceleration time history and pseudo-velocity response spectrum of input seismic motions

the weight for the x and y directions. Contact-type displacement meters were installed on each leaf spring to measure the story drift of the frame, and a laser displacement meter was installed on a bracket attached to the steel plate in order to measure the relative displacement (sliding displacement) between the frame and the weight. The maximum story drift of the frame in the following graphs was defined as the mean value of the maximum drifts obtained from the four leaf springs.

B. Experimental Parameters

The four experimental parameters of interest are as follows: (1) the yield shear force coefficient of the frame C_y , (2) the dynamic friction coefficient of the weight μ_d , (3) the

maximum velocity of the input seismic motion V_{max} , and (4) the weight-to-frame mass ratio R_m (Table I).

The yield shear force coefficient C_y in the present study is the ratio of the yield strength of the frame Q_{yf} to the frame mass, including the mass of the weight. Then, by adjusting the tightening torque T_h of the frame, C_y became 0.248, 0.314, 0.413, and 0.612. However, the results for $C_y = 0.248$ are presented in the following. In addition, T_h was adjusted to be sufficiently large ($C_y = \infty$) for the purpose of comparison with the elastic response of the frame.

The dynamic friction coefficients at the interface of the weight and the steel plate of the frame μ_d were calculated based on the horizontal forces obtained through a static sliding experiment involving the weight for various sliding materials adhered to the bottom of the weight. Based on the sliding experiment, three types of sliding materials were

selected: polytetrafluoroethylene ($\mu_d = 0.100$), ultra-high-molecular-weight polyethylene ($\mu_d = 0.188$), and natural rubber ($\mu_d = 0.435$).

The maximum velocity of the input seismic motion V_{max} was set based on the assumption of a range of from moderate earthquake motion ($V_{max} = 0.2$ m/s) to extremely rarely occurring earthquake motion ($V_{max} = 0.5$ m/s) in 0.1-m/s increments.

By adjusting the number of weights (1-ply = 2.08 kg) to 5-, 10-, and 15-ply, the weight-to-frame mass ratio R_m varied as 0.219, 0.438, and 0.657, respectively. The primary natural

periods of the frame with fixed weights are 0.173 s (5.77 Hz), 0.184 s (5.44 Hz), and 0.200 s (5.00 Hz).

C. Selected Input Seismic Motions

The three seismic motions used in the present study, which have relatively larger maximum acceleration and different predominant periods, observed in Japan, were standardized according to maximum velocity (Fig. 3). These three seismic motions: (a) HYG024_2013_EW ((a) HYG), (b) KMM008_2016_EW ((b) KMM), and (c) ISK005_2007_EW ((c) ISK), were observed in Higasiura, Hyogo (2013), Uto, Kumamoto (2016), and Anamizu, Ishikawa (2007), respectively.

III. EXPERIMENTAL RESULTS FOR THE PARAMETERS

A. Maximum Response of the Frame and Weight for the Dynamic Friction Coefficient

Fig. 4 shows the response results of the frame and the weight for the dynamic friction coefficient μ_d for each input seismic motion (experimental parameters: $C_y = 0.248$, $V_{max} =$

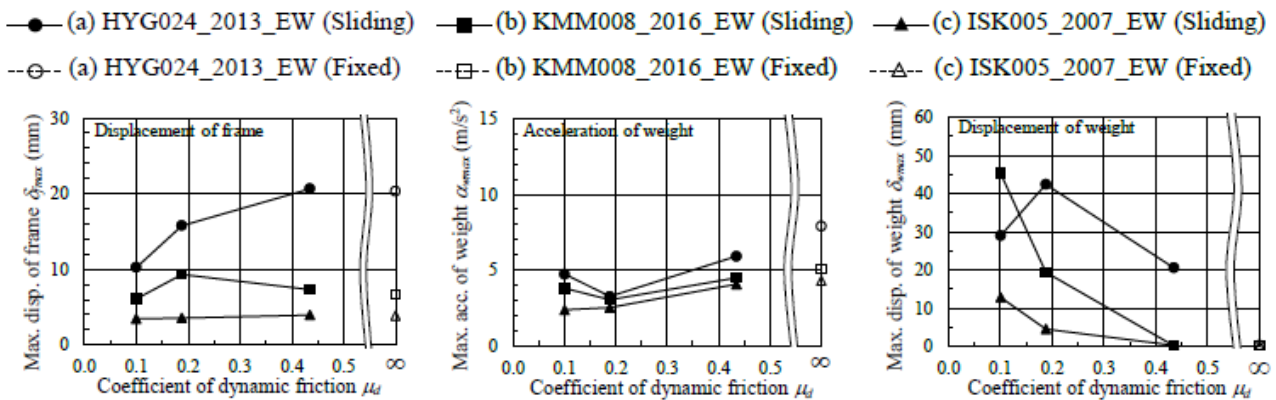


Fig.4 Relationship between μ_d and maximum response of the frame and weight
[$C_y = 0.248$, $V_{max} = 0.4$ m/s, $R_m = 0.438$]

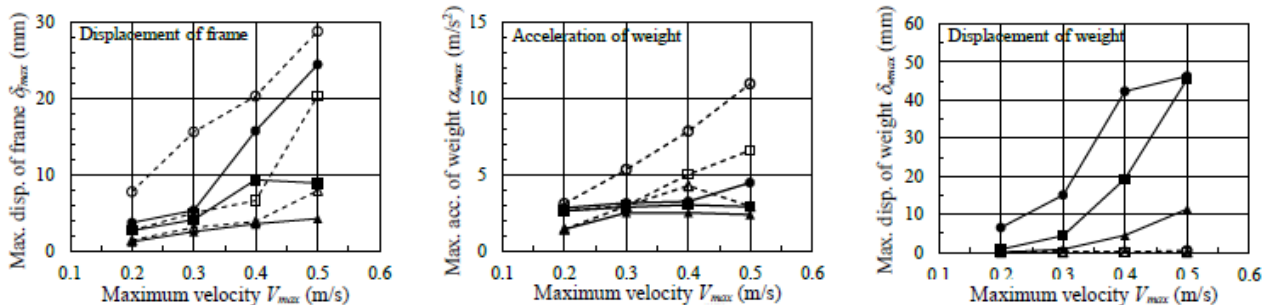


Fig.5 Relationship between V_{max} and maximum response of the frame and weight
[$C_y = 0.248$, $\mu_d = 0.188$, $R_m = 0.438$]

0.4 m/s, and $R_m = 0.438$). The graph on the left shows the maximum story drift of the frame δ_{fmax} , and the middle graph shows the maximum response acceleration of the weight α_{wmax} . Moreover, the right-hand graph shows the maximum

sliding displacement of the weight α_{wmax} . The symbols in the fig. indicate the results for the input seismic motions: (a) HYG (circle), (b) KMM (square), and (c) ISK (triangle). The symbol ∞ on the horizontal axis indicates the results for the case in which the weight is fixed.

Although there is a slight variation in the maximum story drift of the frame δ_{fmax} (left-hand graph), δ_{fmax} decreases as μ_d decreases. As shown in the left-hand graph, α_{wmax} increases in the order of the input seismic motion, i.e., (c) ISK, (b) KMM, and (a) HYG, because δ_{fmax} may increase by the seismic motion for which the predominant period is close to the primary natural period of the frame. The maximum response acceleration of the weight α_{wmax} (middle graph) decreases with decreasing μ_d for all input seismic motions except for $\mu_d = 0.100$. In particular, for the case of (a) HYG for $\mu_d = 0.188$, α_{wmax} was reduced by approximately 59% compared to the 0.248, $\mu_d = 0.188$, and $R_m = 0.438$). The solid and dashed lines indicate the response results for the sliding weight (Sliding) and the fixed weight (Fixed), respectively.

Although there is a slight variation in the maximum story drift of the frame δ_{fmax} (left-hand graph), δ_{fmax} increases as V_{max} increases. The slide effect can be observed in the left-hand graph because δ_{fmax} of the sliding weight is lower than that of the fixed weight, except for the case of (b) KMM for $V_{max} = 0.4$ m/s. The maximum response acceleration of the weight α_{wmax} (middle graph) increases with increasing V_{max} in the Sliding case, and is essentially constant with increasing V_{max} in the Fixed case. This difference in α_{wmax} between the Sliding and Fixed cases increases with increasing V_{max} , indicating that the slide effect is significant. The maximum sliding displacement of the weight α_{wmax} (right-hand graph)

case in which the weight was fixed. The maximum sliding displacement of the weight α_{wmax} (right-hand graph) increases with decreasing μ_d , except for the case of (a) HYG for $\mu_d = 0.100$. Therefore, δ_{fmax} and α_{wmax} decrease with decreasing μ_d and α_{wmax} increases with decreasing μ_d .

B. Maximum Response of the Frame and Weight for the Maximum Velocity of the Seismic Motion

Fig. 5 shows the response results of the frame and the weight for the maximum velocity of the input seismic motion V_{max} for each input seismic motion (experimental parameters: $C_y =$ shows that α_{wmax} increases with increasing V_{max} for all input seismic motions. Thus, the slide effect increases with increasing α_{wmax} for μ_d and V_{max} . Therefore, the influence of α_{wmax} is significant for the slide effect.

C. Response Reduction Ratio of the Frame and Weight for Cumulative Sliding Displacement

In the previous section, the slide effect was determined to be related to the maximum sliding displacement of the weight. Therefore, the cumulative sliding displacement of the weight δ_{wcum} was calculated from the time history waveform of the sliding displacement in order to obtain the relationship between the Sliding-to-Fixed displacement ratio of the frame R_{df} and δ_{wcum} (Fig. 6(i)) and the relationship between the Sliding-to-Fixed acceleration ratio of the weight R_{aw} and δ_{wcum} (Fig. 6 (ii)). The symbols in the fig. indicate the results

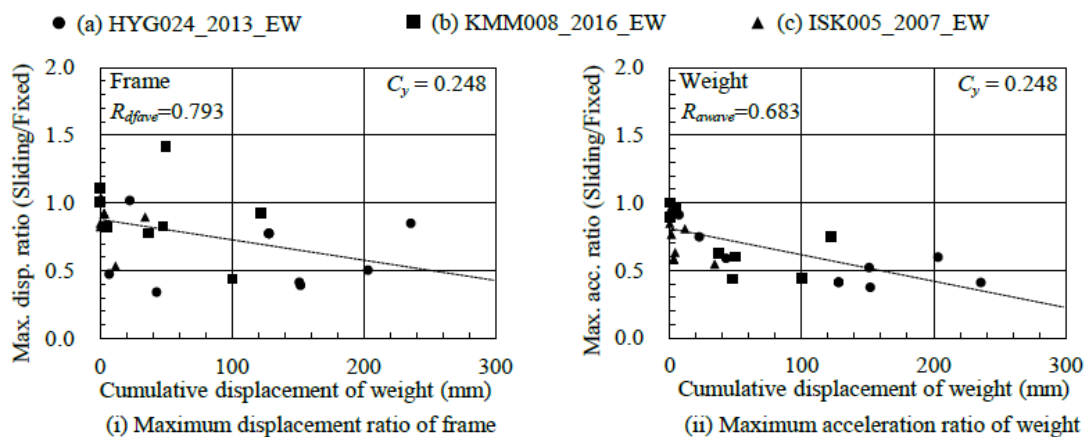


Fig.6 Relationship between cumulative displacement of weight and maximum response ratio of sliding to fixed

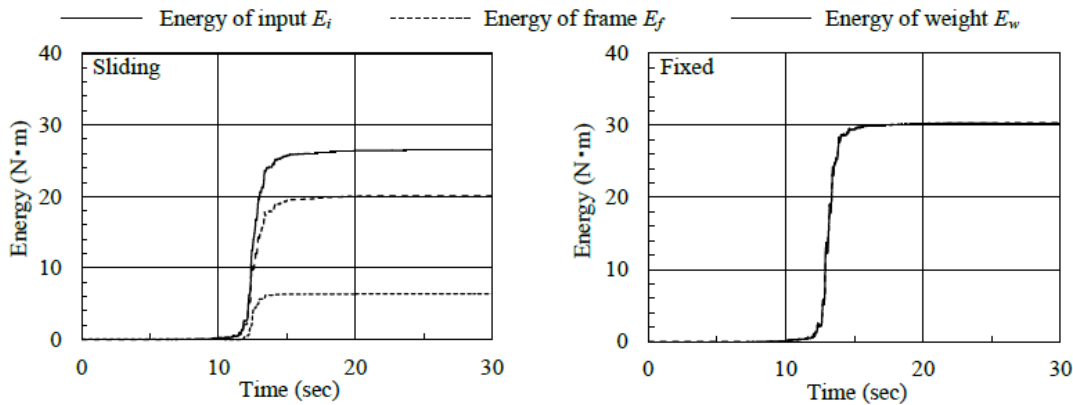


Fig.7 Time histories of experimental energy for the input, frame, and weight calculated by using (3) and (4) [(a) HYG024_2013_EW, $C_y = 0.248$, $\mu_d = 0.188$, $V_{max} = 0.4$ m/s, $R_m = 0.438$]

for the input seismic motions: (a) HYG (closed circle), (b) KMM (closed square), and (c) ISK (closed triangle). The slide effect can be confirmed if R_{df} and R_{aw} are less than 1.0. The dashed line in Fig. 6 is a regression line, R_{dfave} and R_{awave} are the mean values of R_{df} and R_{aw} , respectively. In some cases, R_{df} was more than 1.0, however, the slide effect was generally observed (i). R_{aw} was generally 1.0 or less, therefore, the slide effect was confirmed (ii). The regression lines for R_{df} and R_{aw} tend to decrease with increasing δ_{wcum} , and it is clear that the slide effect increases with increasing δ_{wcum} .

D. Vibration Absorption Energy of the Frame and Weight

The absorption energy due to the plastic deformation of the frame and the sliding of the weight is calculated in this section. The response shear forces of the frame Q_f and the weight Q_w were calculated from the product of these masses and the response acceleration of the frame and the weight:

$$Q_f = -m_f \ddot{x}_f - m_w \ddot{x}_w \quad (1)$$

$$Q_w = -m_w \ddot{x}_w \quad (2)$$

where m_f and m_w are the masses of the frame and the weight, respectively, and \ddot{x}_f and \ddot{x}_w are the absolute accelerations of the frame and the weight, respectively. The absorption energy of the frame E_f was calculated as the product of Q_f and

the story drift, and the weight E_w was calculated as the product of Q_w and the sliding displacement, as follows:

where x_f and x_w are the story drift of the frame and the sliding displacement of the weight, respectively. The input energy E_i is the sum of E_f and E_w .

Fig. 7 shows the time history waveforms of absorption energy E_f and E_w in the cases of a sliding weight (Sliding) and a fixed weight (Fixed), respectively (experimental parameters: (a) HYG, $C_y = 0.248$, $\mu_d = 0.188$, $V_{max} = 0.4$ m/s, and $R_m = 0.438$). Since the sliding displacement in the Fixed case is approximately 0, E_w is also negligible. Therefore, E_i and E_f are equal. In contrast, E_d appears in the Sliding case because the weight slides on the steel plate of the frame. Thus, the ratio of the absorption energy of the frame to the input

$$E_f(t) = \int_0^t Q_f x_f dt \quad (3)$$

$$E_w(t) = \int_0^t Q_w x_w dt \quad (4)$$

where x_f and x_w are the story drift of the frame and the sliding displacement of the weight, respectively. The input energy E_i is the sum of E_f and E_w .

Fig. 7 shows the time history waveforms of absorption energy E_f and E_w in the cases of a sliding weight (Sliding) and a fixed weight (Fixed), respectively (experimental parameters: (a) HYG, $C_y = 0.248$, $\mu_d = 0.188$, $V_{max} = 0.4$ m/s, and $R_m = 0.438$). Since the sliding displacement in the Fixed case is approximately 0, E_w is also negligible. Therefore, E_i and E_f are equal. In contrast, E_d appears in the Sliding case because the weight slides on the steel plate of the frame.

International Journal of Engineering Research in Mechanical and Civil Engineering (IJERMCE)
Vol 2, Issue 9, September 2017

Thus, the ratio of the absorption energy of the frame to the input

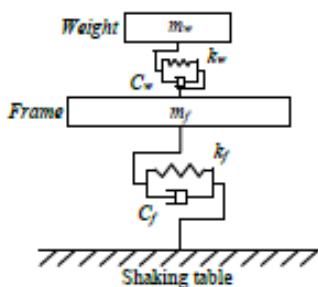


Fig.8 Analytical model

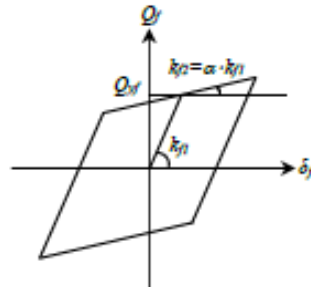


Fig.9 Bilinear model of the frame

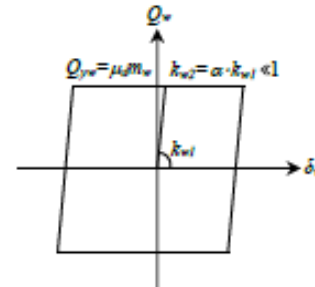


Fig.10 Bilinear model of the weight

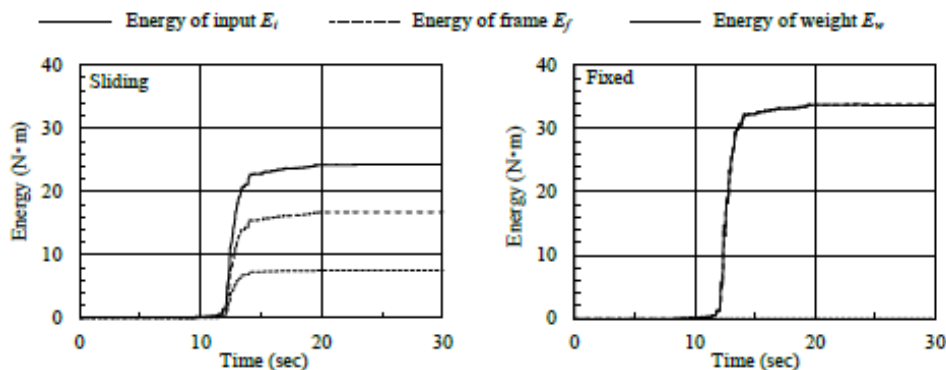


Fig.11 Time histories of analytical energy for the input, frame, and weight calculated by using (3) and (4) [(a) HYG024_2013_EW, $C_f = 0.248$, $\mu_d = 0.188$, $V_{max} = 0.4\text{m/s}$, $R_m = 0.438$]

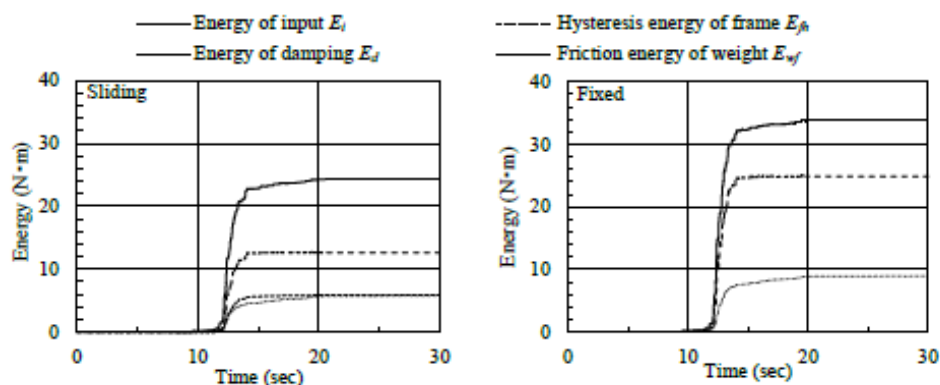


Fig.12 Time histories of each energy involving hysteresis and damping energy [(a) HYG024_2013_EW, $C_f = 0.248$, $\mu_d = 0.188$, $V_{max} = 0.4\text{m/s}$, $R_m = 0.438$]

energy was found to decrease due to the occurrence of E_w by the sliding of the weight, and the input energy decreases by the slide effect. The absorption energy includes the damping

energy because the absorption energy was calculated based on the shear force obtained from the acceleration of the experimental results. Therefore, analytical study is necessary

in order to obtain the hysteresis energy (friction energy) by only the friction force of the weight.

input energy, the hysteresis energy of the frame, and the friction energy of the weight were calculated analytically for the purpose of comparison with the energy obtained from the experimental results. The damping energy was also estimated

IV. SEISMIC RESPONSE ANALYSIS CONSIDERING THE SLIDE EFFECT

A. Analytical Model

It is clear that the slide effect is considerably related to the friction energy due to the sliding weight. In this section, the

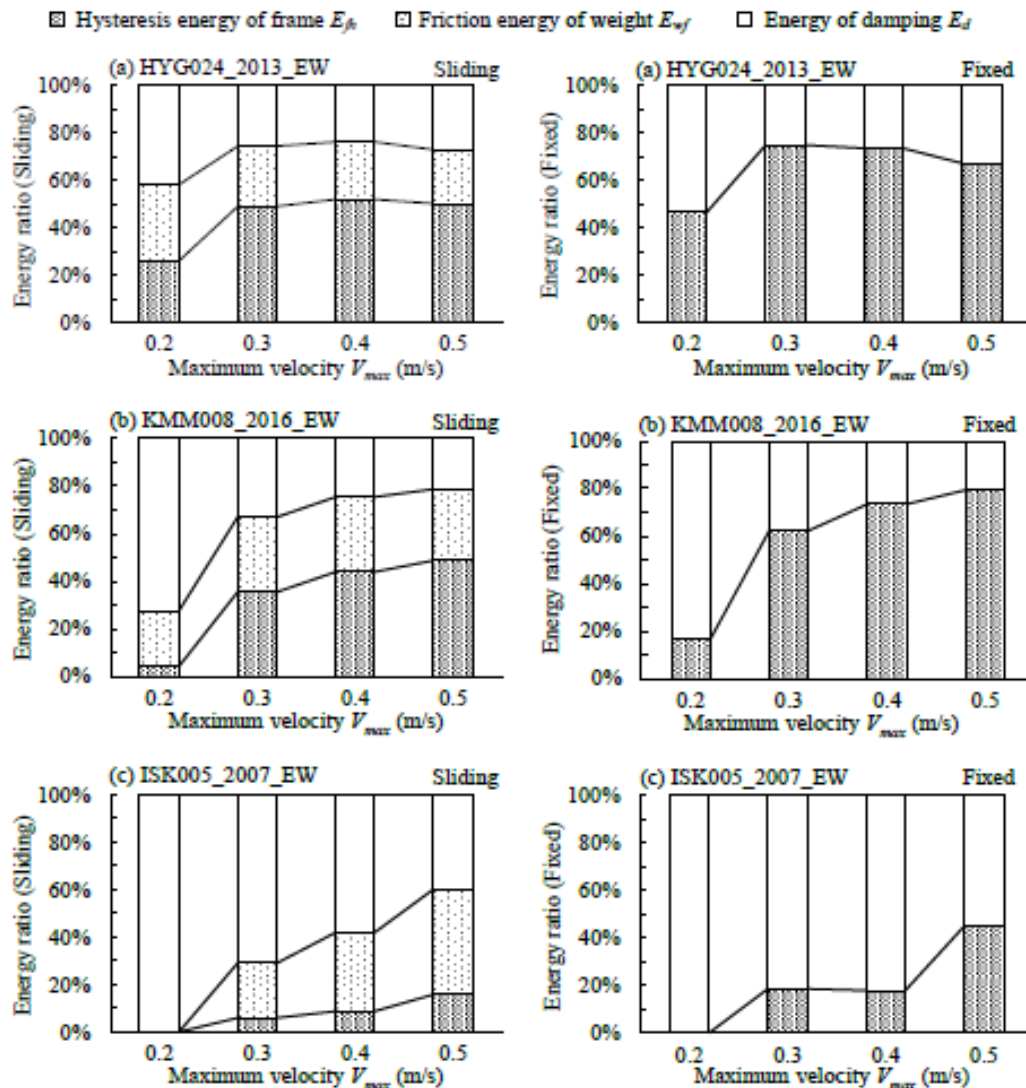


Fig.13 Analytical energy ratio of frame, weight, and damping
[$C_d = 0.248, \mu_w = 0.188, R_m = 0.438$]

in order to discuss the ratio of each energy to the input energy after confirming the validity of the analytical model based on the experimental results.

The analytical model consists of an elastoplastic two-degree-of-freedom system with the mass of the frame m_f and the mass of the weight m_w (Fig. 8). The restoring force characteristics for the frame and the weight sliding are bilinear models, as shown in Figs. 9 and 10, respectively. The initial stiffness k_{f1} , the second stiffness k_{w2} , and the yield shear force Q_{yf} of the frame were obtained from static cyclic loading tests, which were conducted separately. The initial stiffness k_{f1} , the second stiffness k_{w2} , and the dynamic friction force Q_{yw} of the weight were estimated by free vibration tests and sliding tests. The second stiffness of the weight k_{w2} during sliding is assumed to be extremely low, and the stiffness lowering rate was set to be 1.0×10^{-6} (a sufficiently small value). The damping was assumed as an initial stiffness proportional damping for each part: $h_f = 4.04\%$ for the frame by the free vibration tests, and $h_w = 0.02\%$ for the weight, according to actual conditions. The Newmark β method ($\beta = 0.25$) was used to obtain the numerical solution, and SNAP Ver. 7 (KOZO SYSTEM) was used in the analyses.

B. Time History Waveform of Energy

The time history waveforms of each energy for the analytical results calculated by using (3) and (4), which are similar to the experimental results, are shown in Fig. 11 (analytical parameters: (a) HYG, $C_y = 0.248$, $\mu_d = 0.188$, $V_{max} = 0.4$ m/s, and $R_m = 0.438$). The analytically obtained energy of the weight E_w is slightly larger than the experimental results shown in Fig. 7. However, the shapes of the waveform are similar. Although the analytical results, including a strongly nonlinear hysteretic behavior associated with load sliding, were not perfectly consistent with the experimental results, the tendencies of the energy ratios for E_i , E_f , and E_w with the slide effect were simulated.

The energies (E_f and E_w) calculated by using (3) and (4) include the damping energy, in addition to the hysteresis energy. Therefore, E_f and E_w were separated into the hysteresis energy of the frame E_{fh} , the friction energy E_{wf} , and the damping energy E_d using the analytical model. Fig. 12 shows the time history waveforms of E_{fh} , E_{wf} , and E_d extracted from Fig. 11. The ratio of damping energy E_d to the input energy E_i is approximately 23.8% for the Sliding case and approximately 26.4% for the Fixed case. Fig. 12 (left-hand graph) indicates that the friction energy of the weight and damping energy are generally equal. In other words, the damping corresponding to the damping ratio $h_l = 4.04\%$ of the frame was added by the slide effect, so that the total

damping ratio of the system estimated by a simple sum is $h_l \cong 8\%$.

C. Energy Ratios for Sliding and Fixed Weights

The response of the elastoplastic system is greatly influenced by the levels of the input seismic motions. In this section, the energy balance of the structural system to the maximum velocity of the input seismic motion V_{max} is obtained. Fig. 13 shows the ratio of each energy at 30 s to V_{max} for each seismic motion (analytical parameters: $C_y = 0.248$, $\mu_d = 0.188$, and $R_m = 0.438$). The ratio of the hysteresis energy of the frame E_{fh} increases with increasing V_{max} , and the ratio of the damping energy E_d decreases with increasing V_{max} . Moreover, the ratio of the friction energy E_{wf} for the Sliding case with increasing V_{max} decreases in (a) HYG, is constant in (b) KMM, and increases in (c) ISK. Here, E_{wf} is strongly influenced by the phase characteristics of the seismic motions; however, E_{wf} fluctuates very strongly with the velocity of the seismic motions. Thus, the friction energy is constant regardless of V_{max} . However, the friction energy is not generated when the weight is not sliding in the case of (c) ISK for $V_{max} = 0.2$ m/s because the weight slides as a result of the seismic motions, which have a certain level of maximum velocity.

V. CONCLUSIONS

Shaking table tests on a single-story elastoplastic steel frame for various parameters were carried out in order to obtain the basic characteristics of the slide effect for the elastoplastic frame. The story drift of the frame and the acceleration of the weights were reduced by the sliding of the weights. Seismic analyses were conducted in order to calculate and discuss the energy balance of the frame, the weight, and the damping. Although the results of the analysis were not in perfect agreement with the experimental results, the tendencies of the energy ratios for each energy were simulated. Considering the analytically obtained energy, the friction energy of the weight is influenced by the phase characteristic of the seismic motions. However, the friction energy was generated by the seismic motions, which have a certain level of maximum velocity, was constant. The friction energy generated by the sliding weight is not small for the input energy, and a certain damping effect of load sliding can be expected for structural design.

REFERENCES

- [1] N. Ogawa, "Seismic response of frame structures with movable loads," Journal of structural and construction engineering, No. 370, pp. 28-39, Dec. 1986. (in Japanese).

[2] K. Takanashi, K. Ohi, G. Hong, and X. Gao, "Analysis and shaking table tests of frame structures with slipping live load: Response analysis and shaking table test of a block load," Proceeding of architectural research meetings, Kanto chapter, Architectural Institute of Japan, Structural system, No. 58, pp. 141-144, June 1987. (in Japanese).

[3] X. Gao and K. Takanashi, "Earthquake responses of structures with sliding floor loads," Journal of structural and construction engineering, No. 409, pp. 107-113, Mar. 1990. (in Japanese).

[4] J. Paul Smith-Pardo, Juan C. Reyes, Oscar A. Ardila-Giraldo, Luis Ardila-Bothia, and J. Nicolas Villamizar-Gonzalez, "Dynamic effect of sliding rigid blocks on the seismic response of structures," Second European Conference on Earthquake Engineering and Seismology, Aug. 2014.

[5] K. Yamagishi, "Study seismic response reduction effect of building by load sliding," Research report of Hokuriku chapter, Architectural Institute of Japan, No. 58, pp. 102-105, July 2015. (in Japanese).

[6] R. Sasaki and K. Yamagishi, "Fundamental experiment of seismic response reduction effect related to the structure using loads slipping, Journal of Structural Engineering, Architectural Institute of Japan, Vol. 63B, pp. 303-316, Mar. 2017. (in Japanese).

[7] R. Sasaki and K. Yamagishi, "Fundamental experiment of seismic response reduction effect of three story steel frame using weights slipping, Research report of Hokuriku chapter, Architectural Institute of Japan, No. 60, pp. 44-47, July 2017. (in Japanese).

[8] K. Takanashi and X. Gao, "Earthquake resistant design of single story frame with sliding floor load, Summaries of technical papers of annual meeting, Architectural Institute of Japan, B, Structures I, pp. 47-48, Sep. 1989. (in Japanese).